One Pot Synthesis of Pineapple Juice Derived - Carbon Quantum Dots and TiO_2 Composite for Solar Light Active Photocatalysis

Lan Ching Sim[a*], Lee Jie Yet[b], Kah Hon Leong[b], Yik Heng Chinb, Pichiah Saravanan[c]

[a]Department of Chemical Engineering, Lee Kong Chian Faculty of Engineering and Science, Universiti Tunku Abdul Rahman, Kajang, Selangor, Malaysia

[b]Department of Environmental Engineering, Faculty of Engineering and Green Technology, Universiti Tunku Abdul Rahman, Kampar, Perak, Malaysia

[c]Department of Environmental Science and Engineering, Indian Institute of Technology(ISM), Dhanbad, Dhanbad-826004, Jharkhand, India

Abstract

CDs/TiO2 composites were prepared using pineapple juice as a green precursor through one pot hydrothermal method. The obtained CDs exhibited green-blue fluorescence under UV radiation and abundant of surface functional groups. The absorption spectra of CDs/TiO2-200 and CDs/TiO2-120 was red shifted towards visible and NIR region after loading with CDs. Pure anatase and graphite phase were detected in CDs/TiO2. Insignificant emission peak was observed when CDs were excited with wavelength above 540 nm which demonstrated the absence of upconversion photoluminescence (UCPL) properties in CDs. Both of CDs/TiO2-200 and CDs/TiO2-120 fully degraded BPA solution in 150 and 180 mins, respectively. The photocatalytic performance of both CDs/TiO2-200 and CDs/TiO2-120 were 2.5 times of that using P25 under solar irradiation. The presence of CDs in TiO2 composite effectively suppressed the charge recombination and enhanced visible and NIR light absorption.

Keywords: carbon quantum dots, TiO2, solar light, Bisphenol A, pineapple, green precursor.

Introduction

Carbon quantum dots (CDs), predominantly consist of amorphous carbon together with nanocrystalline regions of sp^2-hybridized graphitic carbon [1]. The CDs are widely applied in the field of bioimaging and sensing owing to their high photoluminescence, biocompatibility, small size (<10 nm) and low toxicity [2]. Besides, CDs also possess the upconversion PL properties and able to harvest long-wavelength light [3]. These properties formulate them functional in photocatalytic degradation of organic pollutants under the irradiation of natural sunlight. Nevertheless, the reported preparation method of CDs has met several limitations, such as limited spectral efficiency, low product yield, lack of size control, the use of toxic chemicals and high temperature for experiments [4]. For this reason, using green materials as precursor to produce CDs such as orange juice [5], soy milk [6], chitosan [7], urine [8] and orange waste peels [9] caught the attention of numerous researchers in recent year.

There are 20-50% of fruits and vegetables are thrown away due to its short preservative duration in Malaysia. Instead of creating food waste, the fruits could be potentially used as a carbon source to produce value-added CDs. Green materials derived CDs were widely applied in the field of bioimaging [5[,[10], sensing [11[-[12], solar cells [13]. Unfortunately, the obtained CDs showed superior water solubility, limiting their down-to-earth applicability in photocatalysis, especially in aqueous solutions. On the other hand, conventional photocatalyst such as titanium dioxide (TiO_2) and zinc oxide (ZnO) exhibited the poor absorption properties of visible light and fast recombination of charge carriers which lower the photoactivity [14]. Thus, semiconductor photocatalyst such as ZnO was combined with orange waste peels derived CDs to overcome the solubility problem for the degradation of naphthol blue-black azo dye under ultraviolet (UV) irradiation [9].

Green material derived CDs is cost-effective however, their photodegradation efficiency is questionable because limited attempts have been performed using green materials derived CDs in similar domain since foremost discovery by Prasannan and Imae [9]. Furthermore, this approach has not been sustainably adopted because the abundant and renewable natural solar light which is more suitable to boost the performance of visible and NIR responsive CDs was not explored. To the best of our knowledge, this is first attempt using pineapple juice as starting material to prepare CDs. Therefore, our work proposed the combination of TiO_2 photocatalyst with CDs derived from pineapple juice for the photocatalytic degradation of Bisphenol A (BPA) under natural sunlight irradiation. In this work, one pot hydrothermal method was adopted to prepare nanocomposite of CDs and TiO_2. It is expected that the photocatalytic performance could be enhanced by the sensitization of CDs. This helps to diversify sources of energy today by utilizing solar energy as a sustainable resource to drive the photocatalytic degradation of EDCs which is hazardous to human's health.

*Corresponding author.
E-mail address : simcl@utar.edu.my

Experimental

2.1. Materials

All the chemical reagents used were of analytical grade and purity. Titanium (IV) n-butoxide (ChemSoln, > 98%) was used as the chemical modifier and the TiO_2 precursor respectively. Degussa P25 were used for comparison among photocatalysts. Deionized water was used throughout the experiment. Bisphenol A (Sigma Aldrich, ≥ 99%) were served as organic pollutants for photocatalysis. In addition, ethanol (HMBG, 95%), dichloromethane (Sigma Aldrich, ≥ 99.8%), and acetone solution (Sigma-Aldrich) were used in synthesis process of CDs solution.

2.2. One pot synthesis of CDs/TiO_2 composites

CDs were synthesized using the mixture of pineapple juice and ethanol *via* hydrothermal treatment process. The pineapple was bought from local market and pineapple juice was extracted using a blender. 40 ml of pulp-free pineapple juice was mixed with 30 ml of ethanol and stirred gently. The mixture was poured into Teflon-lined-stainless-steel autoclave and heated at 120℃ for 8 h inside oven. The autoclave was removed from the oven and naturally cooled down under the room temperature for 1 h. The resulted dark brown solution was washed with dichloromethane (CH_2Cl_2) and centrifuged at 3000 rpm for 15 min to separate less fluorescence deposit. Finally, acetone [$(CH_3)_2CO$] was added to upper parts of solution and centrifuged at 10,000 rpm for 15 min to obtain highly fluorescent CDs with smaller sizes. For the synthesis of CDs/TiO_2 composite, 50 ml of CDs solution was mixed with 10 ml of titanium (IV) n-butoxide (TBT, ChemSoln, >98%) and the pH was adjusted to 10 with NaOH solution. Then, the mixture was stirred vigorously for 30 min and placed into teflon-lined-stainless-steel autoclave, heated in oven for 3 h at 120℃. The composite was filtered and washed with distilled water and ethanol simultaneously and finally dried overnight using vacuum oven for 80℃. The CDs/TiO_2 composites calcined at 120℃ and 200℃ (temperature ramp rate of 20℃ /min) were denoted as CDs/TiO_2-120 and CDs/TiO_2-200, respectively.

2.3. Characterization

High Resolution Transmission Electron Microscopy (HRTEM, FEI-TECNAI F20) images were obtained at 200 kV. The X-ray powder diffraction (XRD, PANalytical-Empyrean) was conducted to identify the crystalline phase of the composite. Fourier transform infrared (FTIR, Perkin Elmer Spectrum 400 Spectrophotometer) spectra were carried out in the range of 400-4000 cm^{-1} to identify the functional groups present in the composites. X-ray photoelectron spectroscopy (XPS, PHI Quantera II, Ulvac-PHI, Inc.) was used to further clarify the existing functional groups with Al Kα radiation source. Ultraviolet-visible diffuse reflectance spectra (UV-DRS, Shimadzu UV-2600 spectrophotometer) were measured using $BaSO_4$ as a reference in integrating sphere attachment. A Micro-PL/Raman spectroscope (Renishaw, inVia Raman Microscope) was used to acquire the photoluminescence (PL) and Raman spectra with excitation wavelength at 325 nm and 514 nm, respectively. Photoluminescence (PL) spectra of CDs solution were acquired with a PL spectrophotometer (Perkin Elmer LS 55).

2.4. Photocatalytic experiment

The photocatalytic experiments were carried out using BPA as model pollutant. 150 ml solution containing 2 mg/L of BPA were prepared. 0.2 g of sample was added and kept inside dark for 1 h to reach adsorption-desorption equilibrium. The beakers were then placed under sunlight and the samples were collected in 15 minutes interval for 3 h. The average light intensity was 973 x100 lux. The residual BPA concentration was analyzed using High Performance Liquid Chromatography (HPLC, PerkinElmer Flexar) equipped with fluorescence detector and Ascentis C18 column (Supelco Analytical, USA) (15 cm × 4.6 mm × 5 µm). Acetonitrile (ACN) and water were used in the ratio 40:60 as mobile phase at a flow rate of 1.0 ml/min. The excitation and emission wavelength were 226 and 305 nm, respectively.

Results and discussion

The lattice fringes of the composite were found about 0.35 nm and 0.24 nm (Figure 1a), which match up with the (1 0 1) plane of anatase TiO_2 [15] and (1 0 0) in-plane lattice spacing of graphene respectively [16]. The lattice spacing of CDs can be classified as turbostratic carbon which generally known as hexagonal graphite [3]. The synthesized CDs were distributed well with diameter ranging from 4 to 7 nm (Figure 1b) with the average diameter of 5.4 nm.

From Figure 2, it is observed that there is a broader diffraction peak at 26.2° which indicates the CDs graphene structure after the incorporation of CDs into TiO_2 [17]. The hexagonal graphite phase appeared at 26.2° (0 0 2), 42.1° (1 0 0), 44.4° (1 0 1), 53.8° (0 0 4), and 77.1°(1 1 0). The d-spacing between the (0 0 2) planes of 0.34 nm revealed the presence of functional groups on the surface of the marginally graphitic sheets within the CDs [8]. The weak graphitic crystallinity observed in CDs/TiO_2 composites indicates that CDs are amorphous in nature and exhibited marginal graphitic signals. P25 showed the apparent peak at 25.5° and 27.5° corresponding to (1 0 1) and (1 1 0) of anatase and rutile phase, respectively. Pure anatase TiO_2 phase is detected in all CDs/TiO_2 samples with apparent peaks appeared at 25.5° and 48°, corresponding to (1 0 1) and (2 0 0) crystal planes, respectively. XRD peaks attributed to the anatase phase became weaker after incorporating with CDs. This could be due to higher coverage of CDs on TiO_2 since the volume ratio of CDs is higher than TiO_2 precursor.

Both CDs/TiO_2 composites show a broad band at ~3300 cm^{-1} which indicates the appearance of –OH stretch (Figure 3). Besides, the vibration peak at ~2930 cm^{-1} is assigned to stretching vibration of C-H [18]. The stretching bands at 1620 cm^{-1} and 1380

cm^{-1} indicate the presence of C=C and $–COO^–$ functional groups in CDs/TiO_2 [15]. The presence of aromatic C=C stretch with high sp^2 and π-π* transition characteristic contribute to the fluorescence properties of CDs. The additional of C-O stretch at ~1050 cm^{-1} was also observed in CDs/TiO_2 composites [3]. The absorption peaks corresponding to Ti–O–O was identified around 720 cm^{-1}.

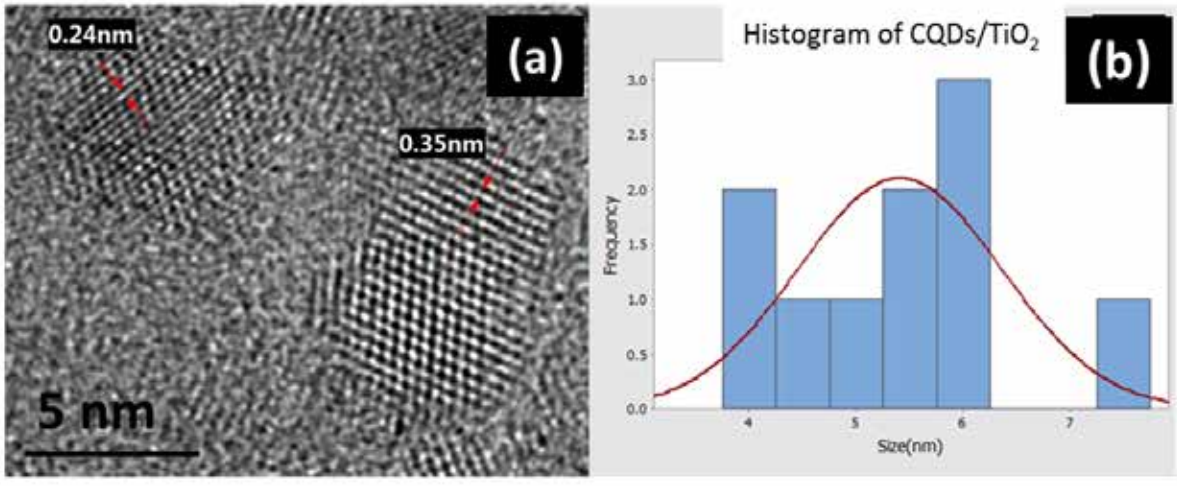

Figure 1 (a) HRTEM image, and (b) size distribution histogram of CDs/TiO_2-120

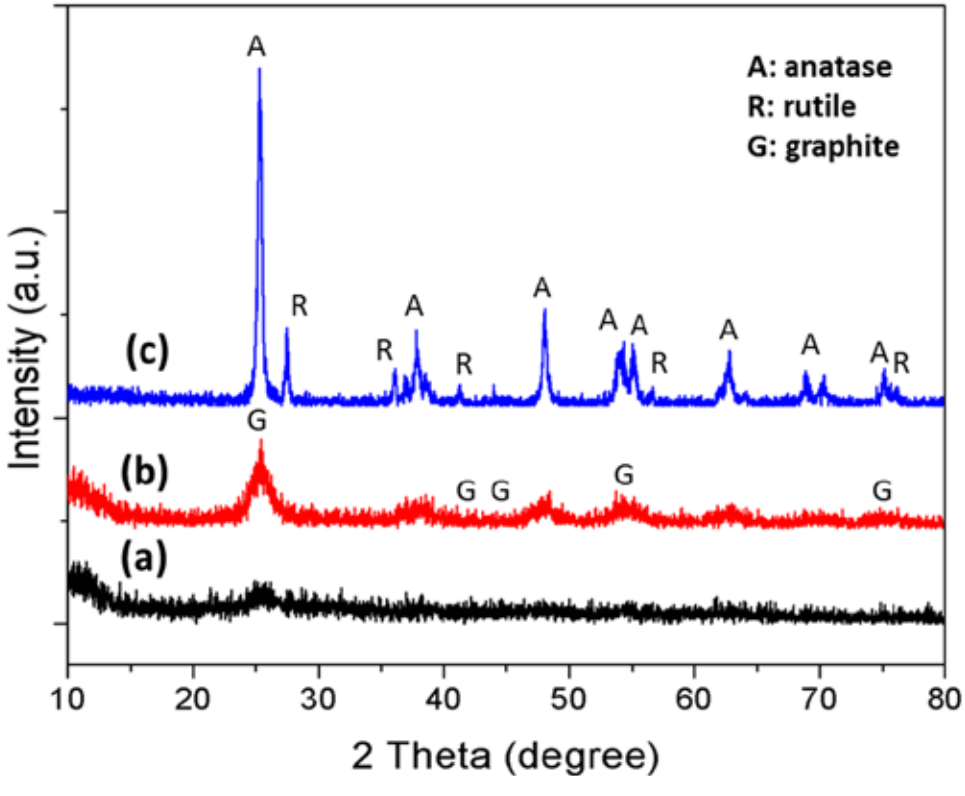

Figure 2 XRD pattern of (a) CDs/TiO_2-200, (b) CDs/TiO_2-120, and (c) P25

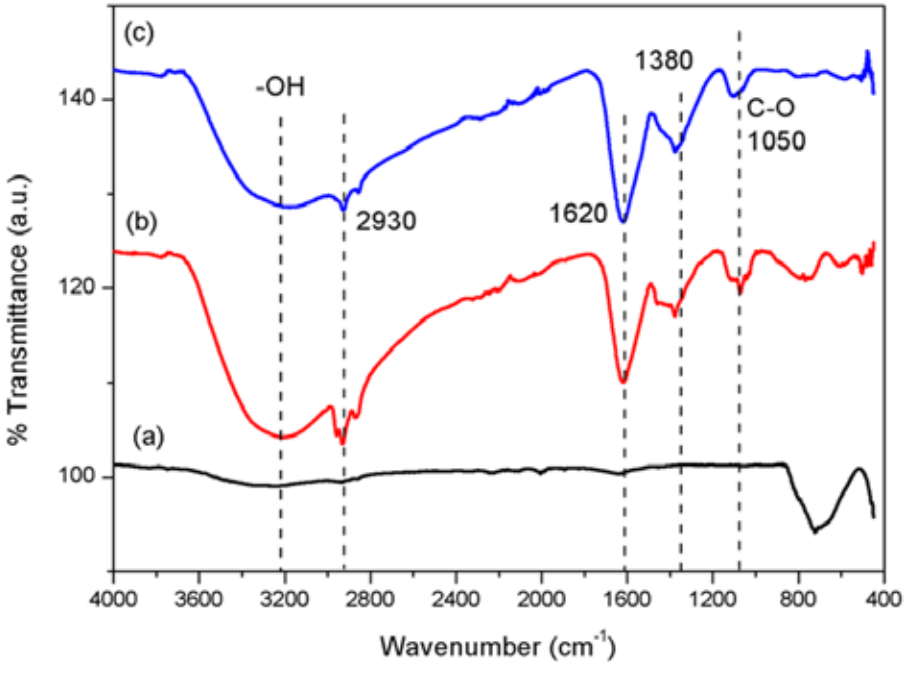

Figure 3 FTIR spectra of (a) P25, (b) CDs/TiO_2-200, and (c) CDs/TiO_2-120.

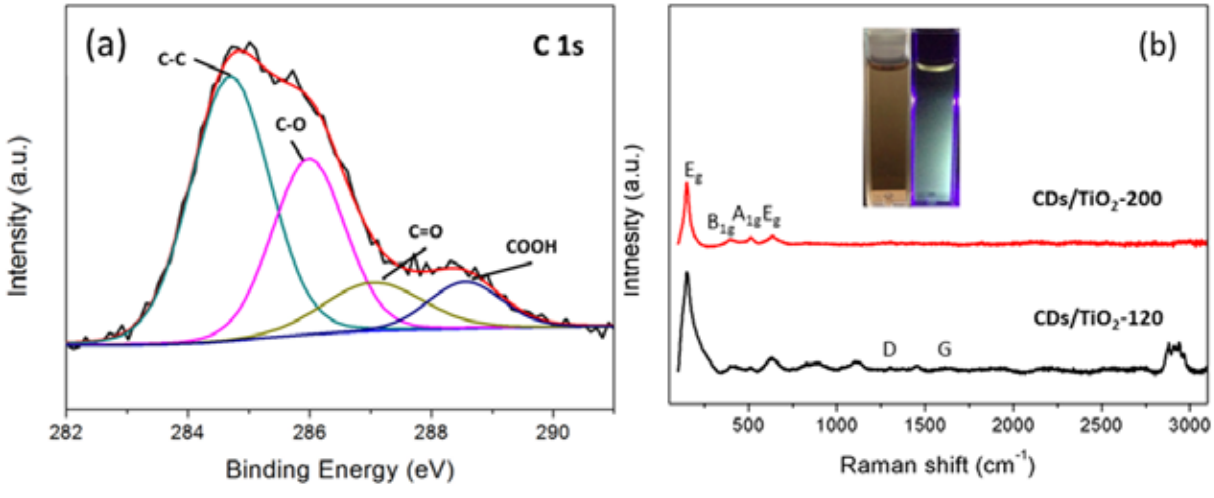

Figure 4 (a) XPS spectra of C 1s for CDs/TiO_2-120, and (b) Raman spectra of prepared samples. Inset shows photograph of CDs solution under daylight (left) and UV light (right).

Figure 4a shows that the core C1s region is deconvoluted into four peaks with binding energy at 284.69, 285.98, 287.04 and 288.55 eV which are assigned for C–C, C–O, C=O and COOH functional groups respectively. This further confirms the presence of COOH and OH groups in the CDs/TiO_2 composites. XPS result also suggests that the hydrothermal treatment can introduce more oxygenated groups like hydroxyl and carbonyl groups into the composites [17]. As shown in Fig. 4b, four distinct Raman peaks of anatase TiO_2 can be observed at about 140 cm^{-1} (E_g), 393 cm^{-1} (B_{1g}), 512 cm^{-1} (A_{1g}) and 637 cm^{-1} (E_g) for prepared samples. This indicates that there was no change in structure properties when CDs were incorporated into TiO_2 [19]. There are two additional peaks that can be observed on CDs/TiO_2 composites at 1585 and 1382 cm^{-1} which represent G and D band respectively. D band represents the carbon atom vibration mode in sp^3 hybridized orbital and also commonly known as defection band which related to present of disorder to the graphene structure. Meanwhile, G band represent the sp^2 vibration mode indicating the presence of graphene in the composite [9],[20]. The presence of D band and G band further proved the existence of CDs in the composites. The inset of Fig. 4b illustrates that the CDs solution exhibited greenish blue fluorescence under 365 nm UV light irradiation while the colour was brown under daylight.

CDs exhibited a dominant peak at about 330 nm (Figure 5a), attributed to π–π* transition of C=C functional groups which is consistent with the FTIR results. Fig. 5b shows that the corresponding PL emission peaks shifted from 430 nm to 550 nm when the CDs were excited at wavelengths ranging from 320 to 540 nm. The PL emission maintained comparable intensities from 320 nm to 380 nm and decreased gradually when the excitation altered from 380 nm to 540 nm. When the excitation wavelength exceeded 500 nm, obvious emission peak is hardly observed, signifying that the PL property of CDs cannot be activated by wavelength above 540 nm. This means that the prepared CDs lack of UCPL properties in which the CDs were not able to convert absorbed NIR light to UV or visible light. The strongest PL peak was located at 470 nm upon 360 nm excitation. The as-prepared CDs demonstrated selective emission colours ranging from blue to green.

As $\frac{c}{\lambda} = f$ $c / l = f$ therefore E=hf and known as 'hv' in chemistry. CDs/TiO_2-200 successfully shows the lowest band gap energy of 2.00 eV compare to that of CDs/TiO_2-120 and P25 with band gap ene rgy of 3.20 eV and 3.30 eV, respectively. This indicates that the hybridization of CDs in higher temperature can improve the visible and NIR light absorption properties of pure TiO_2.

Figure 6c demonstrates the photocatalytic performance of prepared samples towards the degradation of BPA under natural sunlight irradiation. There was no significant adsorption activity occurring in all samples during the adsorption-desorption equilibrium as shown in Figure 6c. All CDs/TiO_2 composites showed higher degradation rate of BPA compared to that of P25 and the blank. The photocatalytic reaction efficiency of BPA followed the sequence of

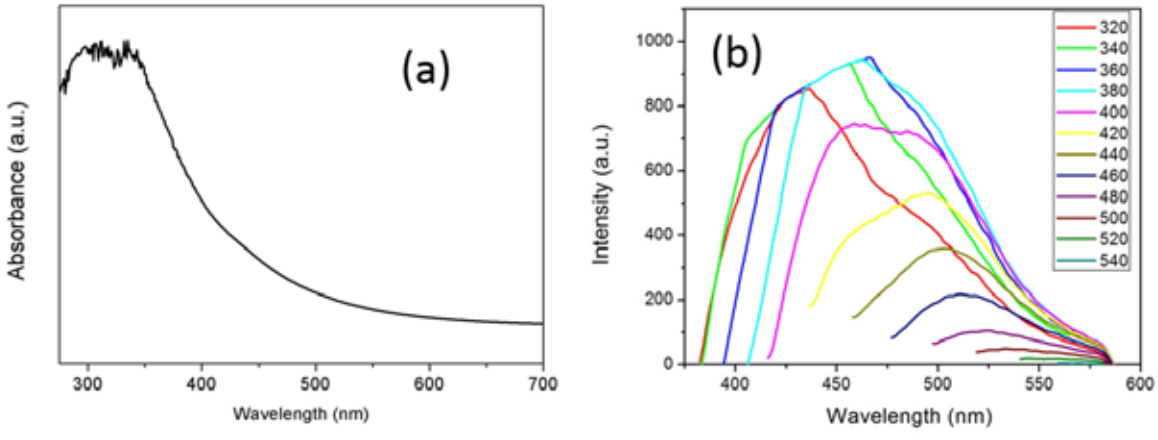

Figure 5 (a) The absorption spectrum of CDs solution and
(b) PL spectra of the CDs with excitation wavelengths ranging from 320nm to 540nm.

As shown in Figure 6a, there is no absorption band in visible region (>400 nm) which fulfil the intrinsic absorption property of P25. The CDs/TiO_2-200 possesses greater potential to harvest entire solar spectrum compared to that of CDs/TiO_2-120. This is proved by the red shifted absorption spectra towards visible and NIR region [21]. The use of higher temperature to synthesize CDs/TiO_2 composite was able to promote the light absorption in full solar spectrum due to the synergistic effects between the surface/molecule state and carbon core [17]. The Tauc plot in Figure 6b was used to study the band gap of the samples. The Kubelka-Munck function, F(R) is derived from the equation below:

$$F(R) = (1 - R)^2/2R \quad (1)$$

where R is the diffuse reflectance, and the band gap is obtained by plotting the graph of $(F(R)*hv)^{1/2}$. The photon energy, E is calculated using the following equation:

$$E(e^v) = hc/x\ (1 - R)^2/2R \quad (2)$$

CDs/TiO_2-200 > CDs/TiO_2-120 > P25> control. The degradation rate of CDs/TiO_2-120 was initially higher than CDs/TiO_2-200 because CDs/TiO_2-120 possessed superior separation of electron hole pairs as proven by its lowest PL intensity in Figure 7a. The significant quenching of PL intensity in CDs/TiO_2 composites indicates that incorporation of CDs into TiO_2 could act as an electron reservoir to trap electrons generated from TiO_2 and thus prolonging the lifetime of charge carriers [18],[22]. However, the degradation efficiency of CDs/TiO_2-200 increased and eventually overtook the performance of CDs/TiO_2-120, achieving 100% removal of BPA after 150 min of reaction time. For CDs/TiO_2-120, BPA was fully degraded after 180 min. Such phenomena suggests that the CDs/TiO_2-200 exhibited strong capability to absorb full solar spectrum from visible to NIR region (Fig. 6a) compared to that of CDs/TiO_2-120, contributing a dominant factor to the great performance towards the end of experiment.

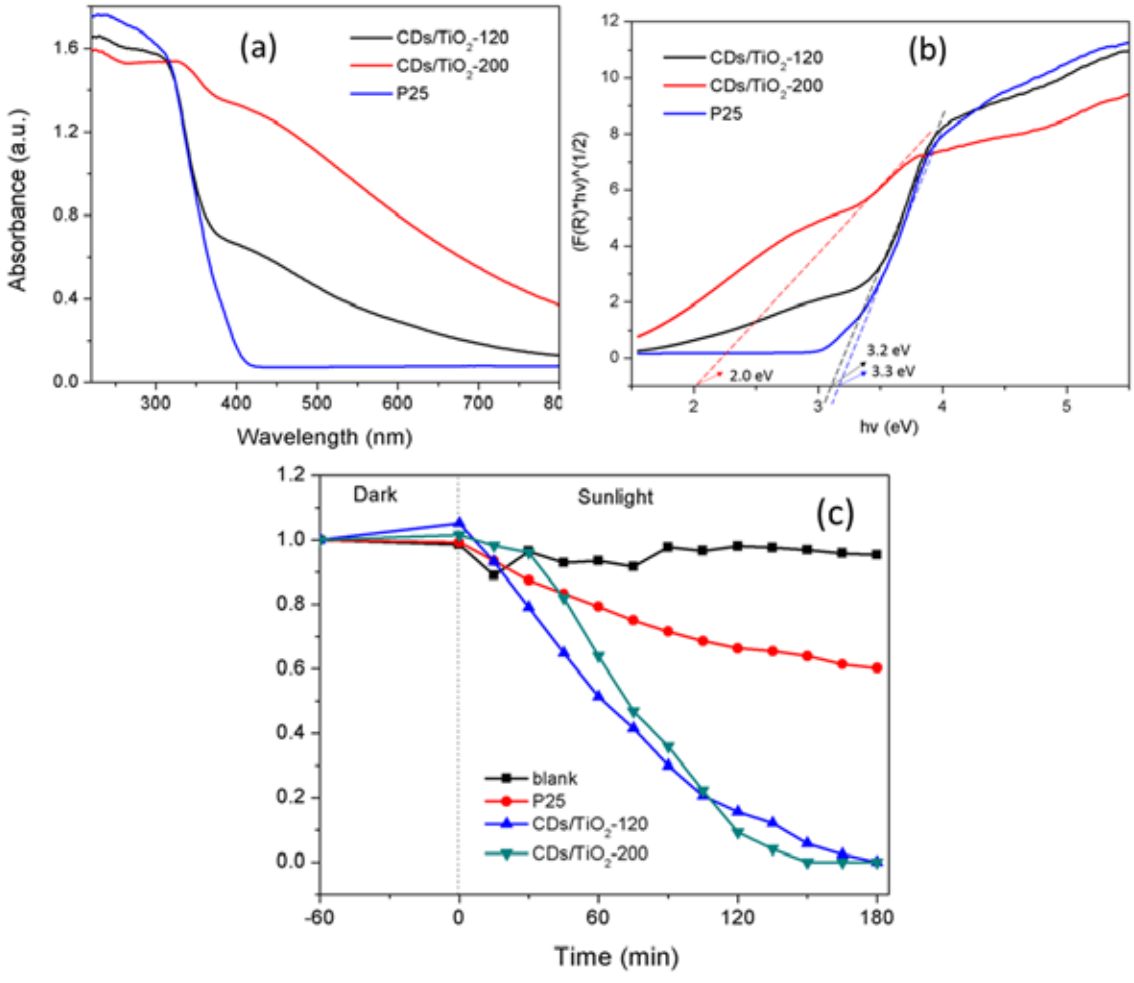

Figure 6 (a) UV-vis absorption spectra, (b) Tauc plot of CDs/TiO_2-120, CDs/TiO_2-200 and P25, and (c) Photocatalytic degradation of BPA as a function of reaction time for prepared samples.

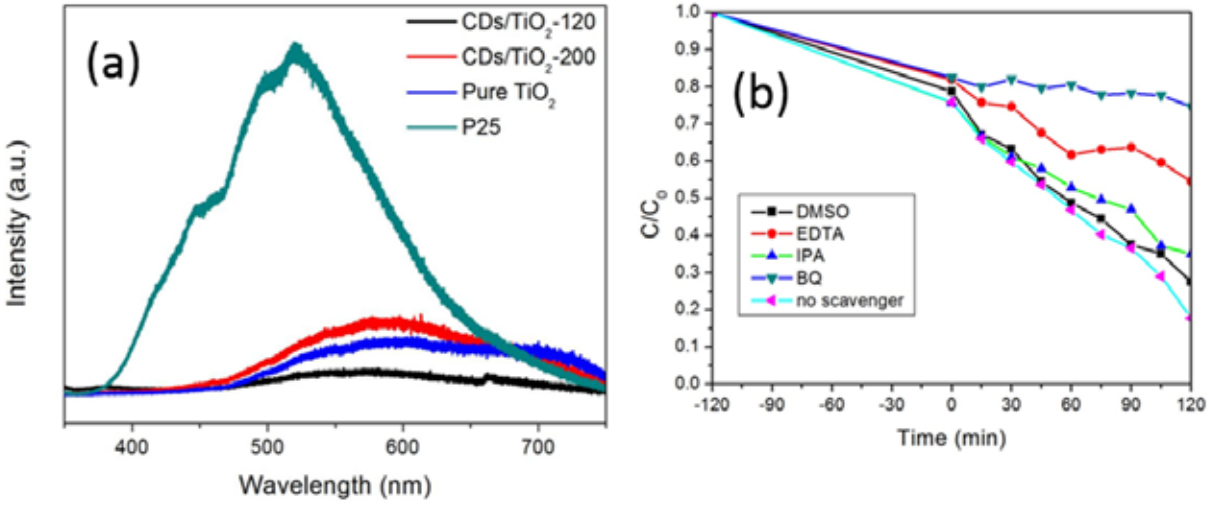

Figure 7 (a) PL spectra of prepared samples and (b) Influence of various radical scavengers on the photocatalytic activity of CDs/TiO_2-200 toward the degradation of BPA under sunlight irradiation.

Figure 7b shows the result of a radical scavenging test which was performed to identify the active radical species responsible for BPA degradation with CDs/TiO_2-200 as photocatalyst. For this test, the reagents used were ethylenediamine tetraacetic acid disodium salt (EDTA-2Na^+), isopropyl alcohol (IPA), dimethylsulfoxide (DMSO) and benzoquinone (BQ) which served as holes (h^+) scavenger, hydroxyl radical ($^•OH$) scavenger, electron (e^-) scavenger and superoxide radical ($^•O^{2-}$) scavenger respectively. The degradation process of BPA was significantly restrained after BQ was added into the mixture solution. This result indicated that $^•OH$ was the most reactive species in the photodegradation process of BPA under sunlight irradiation. The result also revealed that h^+ was the second most reactive radical whereas $^•OH$ and e^- were barely involved in this photocatalysis activity. It is concluded that the most generated radicals in this photocatalytic system follow a sequence of $^•O^{2-} > h^+ > ^•OH > e^-$.

Conclusions

CDs/TiO_2 composites were prepared using one pot hydrothermal method for the removal of BPA. The sensitization of CDs significantly shifted the absorption range of TiO_2 towards the visible and NIR spectrum. Higher temperature up to 200 °C formed a composite with particle size of 5.3 nm which exhibited greater light absorption ability in entire solar spectrum. The presence of CDs in TiO_2 improved the photocatalytic degradation efficiency up to 100% under natural sunlight irradiation. Among the photocatalysts, CDs/TiO_2-200 achieved the fastest rate by degrading 100% of BPA in 150 mins due to its strong capability to absorb entire solar spectrum. CDs/TiO_2-120 showed a better improvement in the separation of electron-hole pairs compared to that of CDs/TiO_2-200, but its lower absorption spectrum slowed down the photoreaction. The key radical species involved in the photoreaction was $^•O^{2-}$. This work provides a new insight for the improvement of conventional photocatalyst without noble metal loading for utilizing solar energy more efficiently.

Acknowledgments

This work was supported by the Universiti Tunku Abdul Rahman Research Fund (IPSR/RMC/UTARRF/2015-C2/S05).

References

[1] S. Lim, W. Shen & Z. Gao, "Carbon quantum dots and their applications," *Chemical Society Reviews*, 44, pp. 362-381, 2015.

[2] F. Wang, Y.H. Chen, C.Y. Liu & D.G. Ma, "White light-emitting devices based on carbon dots' electroluminescence," *Chemical Communications*, 47, pp. 3502-3504, 2011.

[3] J. Wang, Y.H. Ng, Y.F Lim & G.W. Ho, "Vegetable-extracted carbon dots and their nanocomposites for enhanced photocatalytic H_2 production," *RSC Advances,* 4, pp. 44117-123, 2014.

[4] H. Ming, Z. Ma, Y. Liu, K. Pan, H. Yu, F. Wang & Z. Kang, "Large scale electrochemical synthesis of high-quality carbon nanodots and their photocatalytic property," *Dalton Transactions*, 41, pp. 9526-531, 2012.

[5] S. Sahu, B. Behera, T.K. Maiti & S. Mohapatra, "Simple one-step synthesis of highly luminescent carbon dots from orange juice: application as excellent bio-imaging agents," *Chemical Communications*, 48, pp. 8835-837, 2012.

[6] C. Zhu, J. Zhai & S. Dong, "Bifunctional fluorescent carbon nanodots: green synthesis via soy milk and application as metal-free electrocatalysts for oxygen reduction," *Chemical Communications*, 48, pp. 9367-369, 2012.

[7] Y. Yang, J. Cui, M. Zheng, C. Hu, S. Tan, Y. Xiao, Q. Yang Q & Y. Liu, "One-step synthesis of amino-functionalized fluorescent carbon nanoparticles by hydrothermal carbonization of chitosan," *Chemical Communications,* 48, pp. 380-382, 2012.

[8] J.B. Essner, C.H. Laber, S. Ravula, L. Polo-Parada & G.A. Baker, "Pee-dots: biocompatible fluorescent carbon dots derived from the upcycling of urine," *Green Chemistry*, 18, pp. 243-250, 2016.

[9] A. Prasannan & T. Imae, "One-pot synthesis of fluorescent carbon dots from orange waste peels," *Industrial & Engineering Chemistry Research,* 52, pp. 15673-678. 2013.

[10] C.V. Rodrigues, J.R. Correa, C.M. Aiube, L.P. Andrade, P.M. Galvão, P.A. Costa, A.L. Campos, A.J. Pereira, G.F. Ghesti, J.F. Felix, I.T. Weber, B.A. Neto & M.O. Rodrigues, "Down-and up-conversion photoluminescence of carbon-dots from brewing industry waste: Application in live cell-imaging experiments," *Journal of the Brazilian Chemical Society*, 26, pp. 2623-628, 2015.

[11] S. Dinç, "A simple and green extraction of carbon dots from sugar beet molasses: Biosensor applications," *Surg Industry*, 141, pp. 560-564, 2016.

[12] Guo Y, Zhang L, Cao F, Leng Y. Thermal treatment of hair for the synthesis of sustainable carbon quantum dots and the applications for sensing Hg^{2+}. Scientific reports 2016;6:35795.

[13] J. Briscoe, A. Marinovic, M. Sevilla, S. Dunn & M. Titirici, "Biomass-derived carbon quantum dot sensitizers for solid-state nanostructured solar cell," *Angewandte Chemie International Edition*, 54, pp. 4463-468, 2015.

[14] A. Yu, Q. Wang, J. Wang, C.T. Chang, "Rapid synthesis of colloidal silver triangular nanoprisms and their promotion of TiO_2 photocatalysis on methylene blue under visible light," *Catalysis Communications,* 90, 75-78, 2017.

[15] F. Li, F. Tian, C. Liu, Z. Wang, Z. Du, R. Li & L. Zhang, "One-step synthesis of nanohybrid carbon dots and TiO_2 composites with enhanced ultraviolet light active photocatalysis," *RSC Advances,* 5, pp. 8389-396, 2015.

[16] L. Tang, R. Ji, X. Cao, J. Lin, H. Jiang, X. Li, K.S. Teng, C.M. Luk, S. Zeng, J. Hao, S.P. Lau, "Deep ultraviolet photoluminescence of water-soluble self-passivated graphene quantum dots," *ACS Nano,* 6, pp. 5102-110, 2012.

[17] C. Shen, Y. Sun, J. Wang & Y. Lu, "Facile route to highly photoluminescent carbon nanodots for ion detection, pH sensors and bioimaging," *Nanoscale,* 6, pp. 9139-147, 2014.

[18] A. Tyagi, K.M. Tripathi, N. Singh, S. Choudhary & R.K. Gupta, "Green synthesis of carbon quantum dots from lemon peel waste: Applications in sensing and photocatalysis," *RSC Advances*, 6, pp. 72423-2432, 2016.

[19] W. Wang, Y. Ni & Z. Xu, "One-step uniformly hybrid carbon quantum dots with high-reactive TiO_2 for photocatalytic application," *Journal of Alloys and Compounds*, 622, pp. 303-308, 2015.

[20] X. Yu, J. Liu, Y. Yu, S. Zuo & B. Li, "Preparation and visible light photocatalytic activity of carbon quantum dots/TiO_2 nanosheet composites," *Carbon*, 68, pp. 718-724, 2014.

[21] A. Qu, H. Xie, X. Xu, Y. Zhang, S. Wen & Y. Cui, "High quantum yield graphene quantum dots decorated TiO_2 nanotubes for enhancing photocatalytic activity," *Applied Surface Science*, 375, pp. 230-241, 2016.

[22] Z. Zhang, T. Zheng, X. Li, J. Xu & H. Zeng, "Progress of carbon quantum dots in photocatalysis applications," *Particle & Particle Systems Characterization*, 33, pp. 457-472, 2016.